



# *In Vitro* and *In Vivo* Exposure-Effect Relationship of Liposomal Amphotericin B against *Aspergillus fumigatus*

Maria Siopi,<sup>a</sup> Johan W. Mouton,<sup>b</sup> Spyros Pournaras,<sup>a</sup> Joseph Meletiadis<sup>a,b</sup>

<sup>a</sup>Clinical Microbiology Laboratory, Attikon University General Hospital, Medical School, National and Kapodistrian University of Athens, Athens, Greece

<sup>b</sup>Department of Medical Microbiology and Infectious Diseases, Erasmus Medical Center, Rotterdam, the Netherlands

**ABSTRACT** *In vitro* pharmacokinetic/pharmacodynamic data of liposomal amphotericin B (L-AMB) were compared with animal data from neutropenic and nonneutropenic models of azole-susceptible and azole-resistant invasive aspergillosis. L-AMB was equally effective. The *in vitro*  $fC_{max}$  (maximum concentration of free drug)/MIC ratio associated with 50% of maximal activity was 0.31 (0.29 to 0.33), similar to that in neutropenic but not nonneutropenic mice (0.11 [0.06 to 0.20]). Simulation analysis indicated that standard L-AMB doses (1 to 3 mg/kg) are adequate for nonneutropenic patients, but higher doses (7.5 to 10 mg/kg) may be required for neutropenic patients for *Aspergillus fumigatus* isolates with MICs of 0.5 to 1 mg/liter.

**KEYWORDS** *Aspergillus fumigatus*, azole resistance, dose optimization, liposomal amphotericin B, neutropenia

The pharmacodynamics (PD) of liposomal amphotericin B (L-AMB) remain relatively poorly understood because of complex pharmacokinetics (PK) that impede the in-depth comprehension of its exposure-response relationship (1). Although high L-AMB doses up to 15 mg/kg have been used (2), in the absence of a clinical dose-response relationship a dose of 3 mg/kg is generally recommended for the treatment of invasive aspergillosis (IA) (1), with an end-of-treatment favorable response of ~40% for probable/proven cases (3). However, neutropenia may affect the clinical response to L-AMB therapy (4). We therefore studied L-AMB PD in an *in vitro* PK/PD model using previously published data of experimental aspergillosis in neutropenic and nonneutropenic animal models and optimized L-AMB therapy simulating human serum concentration-time profiles against azole-susceptible and azole-resistant *Aspergillus fumigatus* isolates in neutropenic and nonneutropenic patients.

Two clinical *A. fumigatus* isolates, a wild-type strain (AZN8196) and an azole-resistant strain harboring the TR<sub>34</sub>/L98H *cyp51A* mutation (V52-35) (5), with voriconazole/AMB CLSI MICs of 0.125/0.25 and 2/0.25 mg/liter, respectively, were studied (6). The MIC of L-AMB was 0.125 mg/liter for both isolates (6). A previously optimized two-compartment dialysis/diffusion closed PK/PD model was used (7, 8). L-AMB was injected in both compartments of the model every 24 h, while the external compartment was covered with aluminum foil to minimize light exposure and placed on a heated (37°C) magnetic stirrer. Drug levels were determined using a microbiological agar diffusion assay as previously described (8). For the preparation of calibration standard samples, stock solution of L-AMB was diluted 1:1 with methanol, heated for 10 min at 65°C to disrupt the liposomes, and then diluted further in RPMI medium (serial 2-fold dilutions) to obtain final concentrations of 8 to 0.015 mg/liter AMB (9). Internal-compartment (IC) samples were treated similarly. Plates were incubated for 24 h, and the diameter of the partial-growth (80%) inhibition zone (fine growth was ignored) was measured because this endpoint gave the largest analytical sensitivity. Because of nonlinearity between inhibition zones and L-AMB concentrations of >1 mg/liter, IC samples with expected

**Citation** Siopi M, Mouton JW, Pournaras S, Meletiadis J. 2019. *In vitro* and *in vivo* exposure-effect relationship of liposomal amphotericin B against *Aspergillus fumigatus*. *Antimicrob Agents Chemother* 63:e02673-18. <https://doi.org/10.1128/AAC.02673-18>.

**Copyright** © 2019 American Society for Microbiology. All Rights Reserved.

Address correspondence to Joseph Meletiadis, [jmeletiadis@med.uoa.gr](mailto:jmeletiadis@med.uoa.gr).

**Received** 3 January 2019

**Returned for modification** 24 January 2019

**Accepted** 23 March 2019

**Accepted manuscript posted online** 8 April 2019

**Published** 24 May 2019

drug levels of  $>1$  mg/liter were first diluted so that the measured concentration would be in the linearity range of the assay. L-AMB was used for the drug assay to quantify all forms of AMB released from L-AMB in the IC (e.g., on contact with fungi, natural release during incubation, preexisting AMB in the vial of clinical formulation). However, inhibition zones of pure AMB using a 100% inhibition endpoint were the same as those of L-AMB using an 80% inhibition endpoint, although lower concentrations were detected in the L-AMB bioassay. The area under the galactomannan index (GI)-time curve ( $AUC_{GI}$ ) was determined as a surrogate marker of fungal growth as previously described (10). All experiments were carried out in duplicate and were independently performed on two different days.

The *in vitro* PK/PD model was evaluated using the previously published *in vivo* results of nonneutropenic and neutropenic murine models of disseminated aspergillosis (11, 12), where mice were infected with the two *A. fumigatus* strains used in the present study and treated intravenously with seven 4-fold-increasing L-AMB doses of 0.004 to 16 mg/kg once daily for 14 days. Based on previous PK studies in neutropenic CD-1 mice, intravenous 10 and 3 mg/kg L-AMB resulted in peak serum total concentrations ( $tC_{max}$ s) of 47.1 and 15.7 mg/liter, respectively, indicating a 1:5 dose: $tC_{max}$  ratio for this dose range (9). The same ratio was used for nonneutropenic mice because neutropenia does not affect L-AMB PK (13). Thus, 4-fold-increasing L-AMB  $tC_{max}$ s of 0.02 to 80 mg/liter were targeted in the *in vitro* PK/PD model simulating the biphasic time-concentration profile observed in mouse serum (9, 14). The *in vitro* exposure-response relationship (percentage growth inhibition versus  $fC_{max}$  [maximum concentration of free drug]/MIC) after 72 h of incubation was compared with the *in vivo* exposure-response curve (percentage survival versus  $fC_{max}$ /MIC) after 14 days of treatment using the extra sum-of-squares F test. Survival data were normalized to span from 0% survival in drug-free controls to 100%. The *in vivo*  $fC_{max}$  was calculated on the basis of the unbound fraction ( $f_u$ ) of AMB in human serum (15). Total AMB in serum of L-AMB-treated subjects was largely liposome associated in steady state, and the percentage of protein binding (PB) of nonliposomal AMB was concentration dependent, following the equation  $PB = 95.3\% - (99.5\% - 95.3\%) \times (1 - e^{0.11 \cdot \text{total AMB}})$  with a maximum  $f_u$  the limit of AMB water solubility of  $\sim 0.8$  mg/liter (15). Data were analyzed using nonlinear regression analysis based on the sigmoidal  $E_{max}$  (maximum effect) model with variable slope described previously (7, 8) with GraphPad Prism 7.0 (GraphPad Software, San Diego, CA). Exposure indices associated with 20% ( $EI_{20}$ ), 50% ( $EI_{50}$ ), and 80% ( $EI_{80}$ ) of maximal activity were also estimated.

To bridge the *in vitro* data with human PK, Monte Carlo simulation analysis was performed using the Normal random number generator function of Excel spreadsheet (MS Office 2007) for 5,000 patients treated with the standard intravenous dosage of 3 mg/kg of L-AMB once daily. In particular, this dosage resulted in a steady-state mean  $\pm$  standard deviation (SD)  $tC_{max}$  in human plasma of  $21.87 \pm 12.47$  mg/liter, which corresponds to an  $fC_{max}$  of  $0.19 \pm 0.11$  mg/liter based on concentration-dependent  $f_u$  of L-AMB in human serum estimated as described above (15, 16). The probability of target attainment (PTA) was calculated for isolates with AMB MICs of 0.03 to 8 mg/liter. In order to find which are the most clinically relevant EIs, the cumulative fractional responses (CFRs) were estimated for a previously published AMB MIC distribution of clinical *A. fumigatus* isolates, with an MIC range of 0.03 to 8 mg/liter and 70% of isolates having MICs of 0.5 to 1 mg/liter (17), and for the standard L-AMB dose of 3 mg/kg previously used for the primary therapy of probable/proven IA in a randomized trial (3). The PTA using the best EI was then calculated for *A. fumigatus* isolates, with CLSI AMB MICs ranging from 0.008 to 8 mg/liter and for L-AMB doses of 1, 3, 5, 7.5, and 10 mg/kg with steady-state  $tC_{max} \pm$  SD ( $f_u$ ;  $fC_{max} \pm$  SD) of  $\sim 10.94 \pm 6.24$  (1.7%;  $0.19 \pm 0.11$ ),  $21.87 \pm 12.47$  (0.86%;  $0.19 \pm 0.11$ ),  $\sim 43.74 \pm 24.94$  (0.53%;  $0.23 \pm 0.13$ , assuming close to linear PK for this dose range),  $115.1 \pm 104.9$  (0.5%;  $0.56 \pm 0.52$ ), and  $164.7 \pm 119.7$  (0.5%;  $0.82 \pm 0.60$ ) mg/liter, respectively (2, 18). To account for adverse events (nephrotoxicity and hypokalemia) that may cause discontinuation of L-AMB therapy and worsen clinical outcome, adjusted PTA (adjPTA) and CFR (adjCFR) were calculated as  $PTA - PTA \times \% \text{ patients with adverse events}$  and  $CFR - CFR \times \% \text{ patients}$

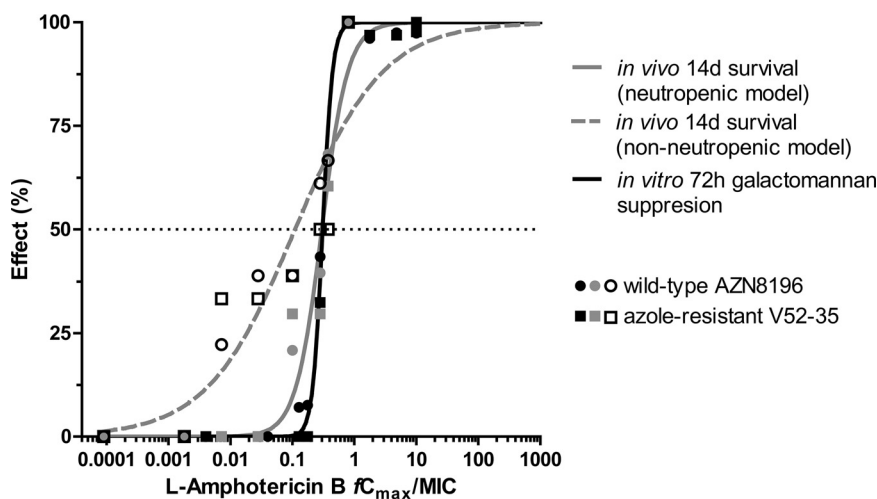


**FIG 1** *In vitro* and *in vivo* PK/PD relationship based on galactomannan suppression and survival rate of experimental nonneutropenic (12) and neutropenic (11) murine models of aspergillosis. *In vitro* PK/PD relationship was similar to *in vivo* PK/PD relationship in neutropenic animal model.

with adverse events, respectively, where the percentage of adverse events was ~2%, 15%, 20%, 25%, and 30% for 1, 3, 5, 7.5, and 10 mg/kg, respectively (2, 4, 19). In addition, the percentage of patients with  $fC_{max}$  higher than the plasma solubility of AMB (~0.8 mg/liter) (15), indicating unnecessary exposure, was calculated for each L-AMB dose.

A biphasic time-concentration profile of L-AMB was simulated in the *in vitro* model attaining the target  $C_{max}$ s and half-life at  $\alpha$  phase ( $t_{1/2,\alpha} \sim 2$  h) but longer  $t_{1/2,\beta}$  (>24 h). After 72 h of incubation, galactomannan production was completely suppressed in both isolates by L-AMB regimens of  $fC_{max} \geq 0.32$  mg/liter. The *in vitro* PK/PD relationship for the two *A. fumigatus* isolates followed a sigmoidal pattern ( $R^2 = 0.99$ ), with mean (95% confidence interval [CI])  $El_{20}$ ,  $El_{50}$ , and  $El_{80}$  of 0.24 (0.22 to 0.26), 0.31 (0.29 to 0.33), and 0.40 (0.34 to 0.46)  $fC_{max}/MIC$  and 2.5 (2.2 to 2.8), 3.6 (3.3 to 4), and 5.3 (4.1 to 6.7)  $fAUC_{0-24}/MIC$ , respectively. The *in vitro* exposure-galactomannan suppression relationship was similar to the *in vivo* exposure-survival relationship of the neutropenic animal model ( $R^2 \geq 0.96$ ) (Fig. 1). The *in vitro*  $El_{50}$  and slope (95% CI) were 0.31 (0.29 to 0.33) and 5.4 (3.03 to 7.80), similar to the *in vivo*  $EC_{50}$  and slope of 0.33 (0.25 to 0.36) and 2.06 (1.11 to 3.09), respectively (extra sum-of-squares F test,  $P = 0.77$ ). No differences were found in the exposure-effect relationship between the two *A. fumigatus* isolates. The *in vivo* exposure-survival relationship in the nonneutropenic animal model followed a sigmoidal pattern ( $R^2 = 0.85$ ), with means (95% CI) of  $El_{20}$ ,  $El_{50}$ ,  $El_{80}$ , and slope of 0.011 (0.003 to 0.038), 0.11 (0.06 to 0.20), 1.06 (0.35 to 3.24), and 0.61 (0.35 to 0.88), respectively (Fig. 1).

Based on Monte Carlo simulation analysis, the CFRs and adjCFRs for  $El_{80}$ ,  $El_{50}$ , and  $El_{20}$  were 34%, 46%, and 59% and 29%, 39%, and 50%, respectively, using the *in vitro* PK/PD targets that correlated with the PK/PD targets in neutropenic mice. Thus, the CFR and adjCFR for  $El_{50}$  were better correlated with the 40% favorable response at the end of treatment (2 weeks) of (mostly neutropenic) patients with proven/probable cases of IA treated with 3 mg/kg of L-AMB in a large randomized clinical trial (3). The proportions of neutropenic and nonneutropenic patients attaining the corresponding  $El_{50}$  targets of 0.31 and 0.11  $fC_{max}/MIC$ , respectively, are shown in Fig. 2. High PTAs (>80%) were found for 1 and 3 mg/kg for isolates with MICs up to 0.25 mg/liter in neutropenic patients and 1 mg/liter in nonneutropenic patients (Fig. 2). The PTAs increased slightly (<16%) with the 5-mg/kg dose for both groups of patients. In neutropenic patients, high CFRs (>81%) were found for isolates with MICs of 0.5 and 1 mg/liter, with 7.5 and 10 mg/kg, respectively. However, because of 20% and 30% adverse events with those doses, respectively, the adjCFR reached only 60%, whereas 20% to 40% of patients will

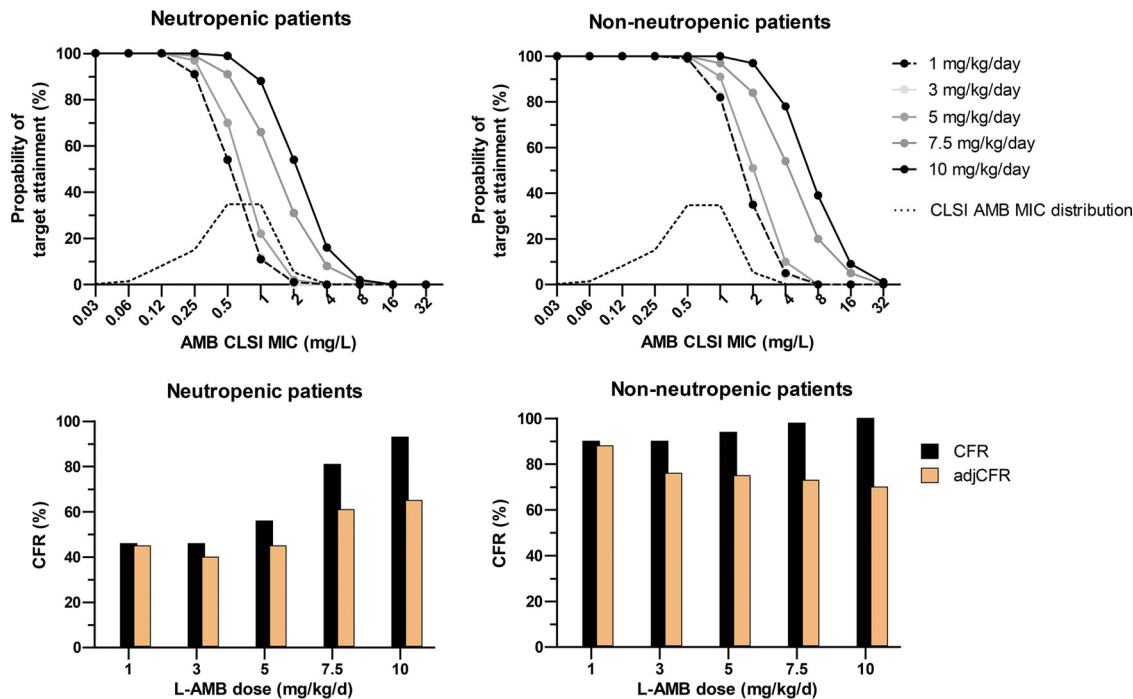


**FIG 2** Probabilities of target attainment of liposomal amphotericin B (L-AMB) monotherapy for *A. fumigatus* isolates with different CLSI AMB MICs and different L-AMB doses in simulated neutropenic and nonneutropenic patients (top). Cumulated fractional response (CFR) adjusted based on adverse events (adjCFR) in simulated neutropenic and nonneutropenic patients (bottom).

be exposed to doses that cannot increase the  $f_u$  of AMB because of the water-solubility limit of 0.8 mg/liter (15). In nonneutropenic patients, the CFR was high (90% to 100%) for all L-AMB doses, including 1 mg/kg, for which the highest adjCFR (88%) was found compared with those at higher doses (70% to 76%).

Although the *in vitro* model was validated using animal data from a model of disseminated aspergillosis rather than a model of pulmonary aspergillosis, which is the most frequent clinical entity, previous studies have shown that the efficacy of L-AMB is similar in these two models, reaching maximal efficacy at  $\geq 10$  mg/kg daily (20, 21). The *in vitro* exposure-response relationship was very similar to the *in vivo* exposure-response relationship in neutropenic mice (Fig. 2), validating the link between *in vitro* L-AMB concentrations measured with the bioassay and the *in vivo* free concentration-dependent  $f_u$  of AMB calculated based on the total (mainly liposomal in steady state) AMB in serum. However, more complex PK phenomena (dose-dependent tissue distribution, concentration-dependent tissue binding, time-dependent tissue accumulation, equilibrium among the different AMB forms in interstitial fluid) cannot be excluded.

*In vivo*, AMB is present as liposome-associated, protein-bound, and free drug, and it is believed that liposome-associated AMB serves as a pool of the other forms of AMB but can also exert antifungal activity by delivering AMB directly to fungal cell membranes (1). The biologically active drug is the free drug together with the AMB released on L-AMB contact with fungi, and this might have been the AMB concentration that was measured with bioassay and exerted its antifungal activity in the *in vitro* model. This may explain the 2-fold-lower MICs of L-AMB compared with MICs of AMB of the isolates in the present study. However, because of spatial and diffusion restrictions *in vivo*, the free  $f_u$  of AMB that diffuses from blood and is released from tissue L-AMB to interstitial fluid is probably exerting the most direct antifungal activity (15). L-AMB in tissues may serve as delivery system that sequesters AMB in interstitial fluid rather than directly into cell membrane of fungi. Indeed immunohistochemistry staining showed that L-AMB was found locally at the sites of infection in the brain but not in close proximity to fungal hyphae (22). In addition, peak L-AMB concentrations in tissue are

usually only 10% of serum concentrations in mouse lung and kidney after i.p. treatment, although accumulation does occur, with tissue trough levels being twice the serum trough levels after 5 days of i.v. treatment (9, 14). Tissue binding of L-AMB in mouse lung, kidney, and liver was estimated to be 1% to 10% (14). In human lungs, autopsy studies showed similar levels (16 h after the last dose on day 10) (23) compared with previously reported serum trough concentrations with the standard dose (16). However, in those studies, tissue homogenates were used where blood and tissue compartments were mixed. Although the bioavailable AMB concentration in tissues (i.e.,  $f_u$  and liposome-associated AMB that reach the fungus in interstitial space) is not known, the low PK/PD index found in the present study and the low response rates found in clinical trials and animal models with the standard dose cannot be explained by the high total or liposome-associated AMB concentration in blood or tissues. Therefore, free AMB is pharmacodynamically more important than total L-AMB concentration, particularly in deep-tissue fungal infections like invasive aspergillosis.

The *in vitro* PK/PD index for L-AMB is higher than the corresponding index for conventional AMB (C-AMB) previously found in the same model (0.31 versus 0.15) (24), indicating that higher L-AMB than C-AMB concentrations are required for the same effect. A similar observation was found in an *in vitro* static model of human alveoli and in animal models, indicating that some of the active compound is locked in the liposome, rendering it inert (25, 26). Interestingly, the PK/PD index of L-AMB determined in the present study ( $tC_{max}/MIC$ , 31, taking into account the  $\sim 1\%$   $f_u$ ) was similar to the PK/PD index determined in the static model ( $tC_{max}/MIC$ , 31.04) in the alveolar compartment where conidia were inoculated and drug diffused into it from the endovascular compartment via the endothelial/alveolar cell lines. This further supports our hypothesis that the *in vitro* model assesses the PD of bioactive diffusible AMB. C-AMB reaches higher free-drug AMB concentrations than L-AMB on a milligram-per-kilogram basis, but its dose-limited nephrotoxicity does not allow for increasing C-AMB doses  $>1$  mg/kg, whereas up to 15 mg/kg of L-AMB has been used with significant toxicity ( $>20\%$ ), observed at doses of  $>5$  mg/kg (2).

L-AMB was equally active against azole-resistant isolates, which align with results in animal models (11) and clinical recommendations for treating azole-resistant aspergillosis (27). Monte Carlo analysis in the present study showed that 1- and 3-mg/kg doses provide similar PTAs. With the caveat of nonlinear L-AMB PK, despite the 2-fold-higher  $tC_{max}$  attained with 3- versus 1-mg/kg doses (22 versus 11 mg/liter, respectively), the unbound AMB value was similar ( $\sim 0.19$  mg/liter) because of the different protein binding (99.14% versus 98.3%, respectively). Indeed, in one of the first clinical trials of L-AMB against IA, the 1-mg/kg L-AMB dose was equally effective to a 4-mg/kg L-AMB dose (clinical response, 64% versus 48%; radiological response, 58 versus 54%, respectively) (4). In that study, the low-dose arm had shorter neutrophil recovery time (14 versus 24 days, respectively) and lower renal toxicity (1% versus 11%, respectively), which might influence clinical outcome. Based on the Monte Carlo analysis of the present study using the nonneutropenic PK/PD target, the adjCFR was higher for the 1-mg/kg dose than for other doses. In neutropenic patients, higher doses up to 10 mg/kg could attain the PD target for almost all wild-type isolates.

These findings are in line with those of animal experiments, where the efficacy of L-AMB was suboptimal in neutropenic mice with  $\sim 30\%$  14-day survival at the standard dose of 3 mg/kg (21) and  $\sim 60\%$  at 10 to 15 mg/kg (28), whereas 1 to 4 mg/kg L-AMB in nonneutropenic mice resulted in 80% survival against isolates with MICs of 0.5 to 1 mg/liter (29). However, high L-AMB doses are associated with a high percentage of adverse events that usually worsen clinical outcome and can result in drug discontinuation. When this toxicity was taken into account, the adjCFR increased only slightly at high doses (up to 60% to 65%, as in animal models). Indeed, clinical trials with high doses ( $\geq 4$  mg/kg) failed to show superiority over lower doses ( $\leq 3$  mg/kg) (3, 4). Given the large PK variation (60% with the standard dose [16] and  $>76\%$  with higher doses [2]) and the narrow therapeutic index, high L-AMB doses may be of benefit for only a subset of neutropenic patients with suboptimal concentrations (e.g.,  $tC_{max} < 30$ ,  $< 15$ ,

and <7.5 mg/liter for isolates with MICs of 1, 0.5, and 0.25 mg/liter, respectively, based on the findings of the present study). Finally, given the water-solubility limit of AMB at 0.8 mg/liter (15), the PK/PD target of  $0.31 fC_{max}/MIC$  could not be attained for isolates with MICs of  $\geq 2$  mg/liter, justifying the clinical susceptibility breakpoint for AMB and *A. fumigatus*. Higher L-AMB doses would not further increase free AMB because of the water-solubility limit, with 20% and 40% of patients treated with 7.5 and 10 mg/kg, respectively, attaining unnecessary drug exposures. Such exposure may be necessary for tissue compartments where L-AMB penetration is poor, e.g., in myocardium and brain (23), although animal models of central nervous system and pulmonary infections showed that high doses (>10 mg/kg) are not more effective (28, 30).

In conclusion, the results of the *in vitro* PK/PD model were comparable to the outcomes of L-AMB therapy *in vivo* in a neutropenic murine model of experimental aspergillosis and in patients with IA. Given the limited treatment options for azole-resistant IA, our results showed that L-AMB has a role in the management of azole-resistant *A. fumigatus* infections because its efficacy against the wild-type isolate and the isolate harboring the azole resistance mechanism was similar. Simulation analysis indicated that a lower than the standard L-AMB dose may be sufficient for nonneutropenic patients without difficult-to-treat infections when toxicity prohibits the use of the standard dose or a step-down dose-reduction approach on neutrophil recovery. However, a higher-than-standard dose may be required, particularly in patients with profound and prolong neutropenia infected with isolates with AMB MICs of 0.5 to 1 mg/liter when low serum L-AMB levels are expected. This hypothesis warrants further clinical verification.

## REFERENCES

- Stone NRH, Bicanic T, Salim R, Hope W. 2016. Liposomal amphotericin B (AmBisome): a review of the pharmacokinetics, pharmacodynamics, clinical experience and future directions. *Drugs* 76:485–500. <https://doi.org/10.1007/s40265-016-0538-7>.
- Walsh TJ, Goodman JL, Pappas P, Bekersky I, Buell DN, Roden M, Barrett J, Anaissie EJ. 2001. Safety, tolerance and pharmacokinetics of high-dose liposomal amphotericin B (AmBisome) in patients infected with *Aspergillus* species and other filamentous fungi: maximum tolerated dose study. *Antimicrob Agents Chemother* 45:3487–3496. <https://doi.org/10.1128/AAC.45.12.3487-3496.2001>.
- Cornely OA, Maertens J, Bresnik M, Ebrahimi R, Dellow E, Herbrecht R, Donnelly JP. 2011. Efficacy outcomes in a randomised trial of liposomal amphotericin B based on revised EORTC/MSG 2008 definitions of invasive mould disease. *Mycoses* 54:e449–e455. <https://doi.org/10.1111/j.1439-0507.2010.01947.x>.
- Ellis M, Spence D, de Pauw B, Meunier F, Marinus A, Collette L, Sylvester R, Meis J, Boogaerts M, Selleslag D, Krcmery V, von Sinner W, MacDonald P, Doyen C, Vandercam B. 1998. An EORTC international multicenter randomized trial (EORTC number 19923) comparing two dosages of liposomal amphotericin B for treatment of invasive aspergillosis. *Clin Infect Dis* 27:1406–1412. <https://doi.org/10.1086/515033>.
- Mavridou E, Bruggemann RJM, Melchers WJG, Verweij PE, Mouton JW. 2010. Impact of *cyp51A* mutations on the pharmacokinetic and pharmacodynamic properties of voriconazole in a murine model of disseminated aspergillosis. *Antimicrob Agents Chemother* 54:4758–4764. <https://doi.org/10.1128/AAC.00606-10>.
- Clinical and Laboratory Standards Institute. 2008. Reference method for broth dilution antifungal susceptibility testing of filamentous fungi; approved standard—2nd ed. CLSI document M38-A2. Clinical and Laboratory Standards Institute, Wayne, PA.
- Siopi M, Mavridou E, Mouton JW, Verweij PE, Zerva L, Meletiadis J. 2014. Susceptibility breakpoints and target values for therapeutic drug monitoring of voriconazole and *Aspergillus fumigatus* in an *in vitro* pharmacokinetic/pharmacodynamic model. *J Antimicrob Chemother* 69:1611–1619. <https://doi.org/10.1093/jac/dku023>.
- Elefanti A, Mouton JW, Verweij PE, Zerva L, Meletiadis J. 2014. Susceptibility breakpoints for amphotericin B and *Aspergillus* species in an *in vitro* pharmacokinetic-pharmacodynamic model simulating free-drug concentrations in human serum. *Antimicrob Agents Chemother* 58:2356–2362. <https://doi.org/10.1128/AAC.02661-13>.
- Chang T, Olson JA, Proffitt RT, Adler-Moore JP. 2010. Differences in tissue drug concentrations following intravenous versus intraperitoneal treatment with amphotericin B deoxycholate or liposomal amphotericin B. *Med Mycol* 48:430–435. <https://doi.org/10.3109/13693780903208249>.
- Al-Saigh R, Elefanti A, Velegraki A, Zerva L, Meletiadis J. 2012. *In vitro* pharmacokinetic/pharmacodynamic modeling of voriconazole activity against *Aspergillus* species in a new *in vitro* dynamic model. *Antimicrob Agents Chemother* 56:5321–5327. <https://doi.org/10.1128/AAC.00549-12>.
- Seyedmousavi S, Mouton JW, Melchers WJG, Verweij PE. 2017. *In vivo* efficacy of liposomal amphotericin B against wild-type and azole-resistant *Aspergillus fumigatus* isolates in two different immunosuppression models of invasive aspergillosis. *Antimicrob Agents Chemother* 61:e02479-16. <https://doi.org/10.1128/AAC.02479-16>.
- Seyedmousavi S, Melchers WJG, Mouton JW, Verweij PE. 2013. Pharmacodynamics and dose-response relationships of liposomal amphotericin B against different azole-resistant *Aspergillus fumigatus* isolates in a murine model of disseminated aspergillosis. *Antimicrob Agents Chemother* 57:1866–1871. <https://doi.org/10.1128/AAC.02226-12>.
- van Etten EW, Otte-Lambillion M, van Vianen W, Kate MT, Bakker-Woudenberg AJ. 1995. Biodistribution of liposomal amphotericin B (AmBisome) and amphotericin B-desoxycholate (Fungizone) in uninfected immunocompetent mice and leucopenic mice infected with *Candida albicans*. *J Antimicrob Chemother* 35:509–519. <https://doi.org/10.1093/jac/35.4.509>.
- Andes D, Safdar N, Marchillo K, Conklin R. 2006. Pharmacokinetic-pharmacodynamic comparison of amphotericin B (AMB) and two lipid-associated AMB preparations, liposomal AMB and AMB lipid complex, in murine candidiasis models. *Antimicrob Agents Chemother* 50:674–684. <https://doi.org/10.1128/AAC.50.2.674-684.2006>.
- Bekersky I, Fielding RM, Dressler DE, Lee JW, Buell DN, Walsh TJ. 2002. Plasma protein binding of amphotericin B and pharmacokinetics of bound versus unbound amphotericin B after administration of intravenous liposomal amphotericin B (AmBisome) and amphotericin B deoxycholate. *Antimicrob Agents Chemother* 46:834–840. <https://doi.org/10.1128/AAC.46.3.834-840.2002>.
- Groll AH, Silling G, Young C, Schwerdtfeger R, Ostermann H, Heinz WJ, Gerss J, Kolve H, Lanvers-Kaminsky C, Vieira Pinheiro JP, Gammelin S,

- Cornely OA, Wuertwein G. 2010. Randomized comparison of safety and pharmacokinetics of caspofungin, liposomal amphotericin B, and the combination of both in allogeneic hematopoietic stem cell recipients. *Antimicrob Agents Chemother* 54:4143–4149. <https://doi.org/10.1128/AAC.00425-10>.
17. Espinel-Ingroff A, Cuenca-Estrella M, Fothergill A, Fuller J, Ghannoum M, Johnson E, Pelaez T, Pfaller MA, Turnidge J. 2011. Wild-type MIC distributions and epidemiological cutoff values for amphotericin B and *Aspergillus* spp. for the CLSI broth microdilution method (M38-A2 document). *Antimicrob Agents Chemother* 55:5150–5154. <https://doi.org/10.1128/AAC.00686-11>.
  18. Hope WW, Goodwin J, Felton TW, Ellis M, Stevens DA. 2012. Population pharmacokinetics of conventional and intermittent dosing of liposomal amphotericin B in adults: a first critical step for rational design of innovative regimens. *Antimicrob Agents Chemother* 56:5303–5308. <https://doi.org/10.1128/AAC.00933-12>.
  19. Cornely OA, Maertens J, Bresnik M, Ebrahimi R, Ullmann AJ, Bouza E, Heussel CP, Lortholary O, Rieger C, Boehme A, Aoun M, Horst H-A, Thiebaut A, Ruhnke M, Reichert D, Vianelli N, Krause SW, Olavarria E, Herbrecht R. 2007. Liposomal amphotericin B as initial therapy for invasive mold infection: a randomized trial comparing a high-loading dose regimen with standard dosing (AmBiLoad trial). *Clin Infect Dis* 44:1289–1297. <https://doi.org/10.1086/514341>.
  20. Olson JA, George A, Constable D, Smith P, Proffitt RT, Adler-Moore JP. 2010. Liposomal amphotericin B and echinocandins as monotherapy or sequential or concomitant therapy in murine disseminated and pulmonary *Aspergillus fumigatus* infections. *Antimicrob Agents Chemother* 54:3884–3894. <https://doi.org/10.1128/AAC.01554-09>.
  21. Barchiesi F, Santinelli A, Biscotti T, Greganti G, Giannini D, Manso E. 2016. Delay of antifungal therapy influences the outcome of invasive aspergillosis in experimental models of infection. *J Antimicrob Chemother* 71:2230–2233. <https://doi.org/10.1093/jac/dkw111>.
  22. Clemons KV, Schwartz JA, Stevens DA. 2012. Experimental central nervous system aspergillosis therapy: efficacy, drug levels and localization, immunohistopathology, and toxicity. *Antimicrob Agents Chemother* 56:4439–4449. <https://doi.org/10.1128/AAC.06015-11>.
  23. Vogelsinger H, Weiler S, Djanani A, Kountchev J, Bellmann-Weiler R, Wiedermann CJ, Bellmann R. 2006. Amphotericin B tissue distribution in autopsy material after treatment with liposomal amphotericin B and amphotericin B colloidal dispersion. *J Antimicrob Chemother* 57:1153–1160. <https://doi.org/10.1093/jac/dkl141>.
  24. Siopi M, Siafakas N, Vourli S, Zerva L, Meletiadiis J. 2015. Optimization of polyene-azole combination therapy against aspergillosis using an *in vitro* pharmacokinetic-pharmacodynamic model. *Antimicrob Agents Chemother* 59:3973–3983. <https://doi.org/10.1128/AAC.05035-14>.
  25. Al-Nakeeb Z, Petraitis V, Goodwin J, Petraitiene R, Walsh TJ, Hope WW. 2015. Pharmacodynamics of amphotericin B deoxycholate, amphotericin B lipid complex, and liposomal amphotericin B against *Aspergillus fumigatus*. *Antimicrob Agents Chemother* 59:2735–2745. <https://doi.org/10.1128/AAC.04723-14>.
  26. Lestner JM, Howard SJ, Goodwin J, Gregson L, Majithiya J, Walsh TJ, Jensen GM, Hope WW. 2010. Pharmacokinetics and pharmacodynamics of amphotericin B deoxycholate, liposomal amphotericin B, and amphotericin B lipid complex in an *in vitro* model of invasive pulmonary aspergillosis. *Antimicrob Agents Chemother* 54:3432–3441. <https://doi.org/10.1128/AAC.01586-09>.
  27. Ullmann AJ, Aguado JM, Arikan-Akdagli S, Denning DW, Groll AH, Lagrou K, Lass-Flörl C, Lewis RE, Munoz P, Verweij PE, Warris A, Ader F, Akova M, Arendrup MC, Barnes RA, Beigelman-Aubry C, Blot S, Bouza E, Brüggemann RJM, Buchheidt D, Cadranet J, Castagnola E, Chakrabarti A, Cuenca-Estrella M, Dimopoulos G, Fortun J, Gangneux JP, Garbino J, Heinz WJ, Herbrecht R, Heussel CP, Kibbler CC, Klimko N, Kullberg BJ, Lange C, Lehrnbecher T, Löffler J, Lortholary O, Maertens J, Marchetti O, Meis JF, Pagano L, Ribaud P, Richardson M, Roilides E, Ruhnke M, Sanguinetti M, Sheppard DC, Sinkó J, Skiada A, Vehreschild M, Viscoli C, Cornely OA. 2018. Diagnosis and management of *Aspergillus* diseases: executive summary of the 2017 ESCMID-ECMM-ERS guideline. *Clin Microbiol Infect* 24:e1–e38. <https://doi.org/10.1016/j.cmi.2018.01.002>.
  28. Olson JA, Schwartz JA, Hahka D, Nguyen N, Bunch T, Jensen GM, Adler-Moore JP. 2015. Toxicity and efficacy differences between liposomal amphotericin B formulations in uninfected and *Aspergillus fumigatus* infected mice. *Med Mycol* 53:107–118. <https://doi.org/10.1093/mmy/myu070>.
  29. Mouton JW, Te Dorsthorst DT, Meis JF, Verweij PE. 2009. Dose-response relationships of three amphotericin B formulations in a non-neutropenic murine model of invasive aspergillosis. *Med Mycol* 47:802–807. <https://doi.org/10.3109/13693780802672644>.
  30. Clemons KV, Espiritu M, Parmar R, Stevens DA. 2005. Comparative efficacies of conventional amphotericin B, liposomal amphotericin B (AmBisome), caspofungin, micafungin, and voriconazole alone and in combination against experimental murine central nervous system aspergillosis. *Antimicrob Agents Chemother* 49:4867–4875. <https://doi.org/10.1128/AAC.49.12.4867-4875.2005>.